J. Fluid Mech. (2006), *vol.* 566, *pp.* 345–355.
doi:10.1017/S0022112006001285 Printed in the United Kingdom

Self-similar dynamics of liquid injected into partially saturated aquifers

By VANESSA MITCHELL[1,2] AND ANDREW W. WOODS[1]

[1]BP Institute for Multiphase Flow, University of Cambridge, Cambridge, CB3 0EZ, UK
[2]Department of Geophysics, Stanford University, Palo Alto, CA 94 305, USA

(Received 12 February 2006 and in revised form 8 May 2006)

The injection of liquid from a central well into a partially saturated aquifer of finite thickness is described using similarity solutions. The solutions illustrate that injection leads to a growing zone around the source in which the fluid fills the whole depth of the aquifer. Beyond this zone, the current adjusts to the depth in the far field as the fluid slumps under gravity. The radial extent of the zone in which the aquifer is fully flooded depends on the ratio of the buoyancy-driven flow speed to the pressure-driven flow speed associated with the injection. New laboratory experiments, using a model porous medium, support the model predictions in the case of an initially unsaturated layer. The analysis is then developed to allow for a fully saturated aquifer, containing fluid of lower density than the injectate, and a further class of similarity solutions is developed. Again, these are shown to be consistent with new laboratory experiments. In concluding, we briefly consider how the results may be combined, to explore the self-similar dynamics of a relatively dense fluid injected into an aquifer which is partially saturated with fluid of smaller density.

1. Introduction

There are many industrial processes in which fluid is injected through a well into a confined subsurface aquifer or permeable rock containing a second miscible fluid. Examples include liquid injection into vapour-dominated geothermal reservoirs (Woods 1999) and shallow storage of fresh water in saline aquifers (Reese 2001). If there is an adverse viscosity contrast across the front or if the rock is highly heterogeneous, then a large dispersive mixed zone can develop between the injected and original fluid (e.g. Henry 1964; Homsy 1987; Menand & Woods 2005). However, if there is a density contrast between the two fluids, and the porous medium is relatively homogeneous, then, as the flow develops, a well-defined nonlinear interface may develop between the original and injected liquid (e.g. Barenblatt 1996; Bear 1972). In this paper, we focus on this latter class of problem in which the gravitational stability of the interface suppresses the dispersion (Menand & Woods 2005) so that we can introduce the simplifying approximation that there is a well-defined front between the two fluids (cf. Huppert & Woods 1995).

We focus on the axisymmetric injection of liquid from a central well into a confined and partially saturated aquifer. We explore the problem theoretically and experimentally, developing a series of similarity solutions which enable us to contrast the motion in a fully unsaturated (figure 1*a*; § 2) and a partially saturated (figure 1*b*; § 3) aquifer. We then briefly turn to injection of a relatively dense fluid into an aquifer of finite thickness which is fully saturated with fluid of smaller density (figure 1*c*; § 4).

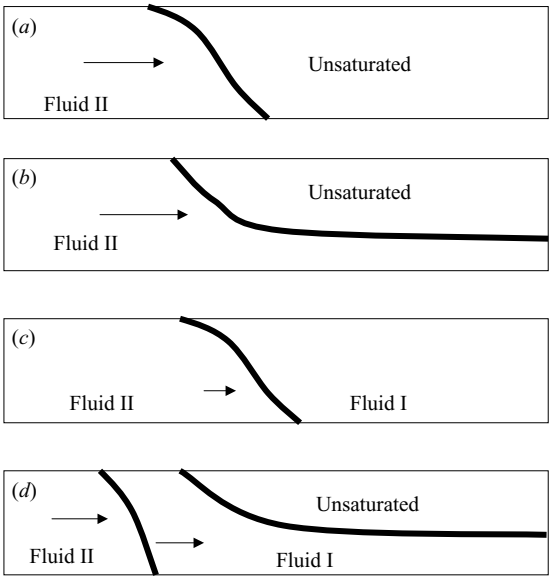

FIGURE 1. Schematic of the motion of a density intrusion into: (*a*) an unsaturated and (*b*) a partially saturated medium with fluid of the same density; (*c*) a fully saturated porous medium with the injection fluid being more dense than the original fluid; and (*d*) a partially saturated porous medium, with the injection fluid being dense than the original fluid.

Finally, we combine the results to make some comments about the displacement of a relatively buoyant fluid which partially fills an aquifer through injection of a relatively dense fluid (figure 1*d*). We conclude by considering the application and relevance of the models to the injection of water into saline aquifers or geothermal reservoirs, and consider the broader application of the work to processes such as water or gas injection in oil reservoirs, in which there may also be effects of immiscibility.

2. Unsaturated layer

We assume liquid of density ρ is injected into a horizontal, laterally extensive unsaturated aquifer of depth H, porosity ϕ and permeability k, with a flow rate Q from a central well (figure 1*a*). By radial symmetry, we expect that the flow properties are simply functions of radius, r, from the well. We assume that once the fluid has spread beyond a distance H from the well, then the pressure becomes hydrostatic (cf. Huppert & Woods 1995) and is given by

$$p(r, z, t) = p_o - \rho g(h - y) \quad \text{for} \quad 0 < y < h, \tag{1}$$

$$p(r, z, t) = p_o \quad \text{for} \quad H > y > h. \tag{2}$$

Using radial symmetry, and Darcy's law for the horizontal component of the flow

$$u = -\frac{k}{\mu}\frac{\partial p}{\partial r} \tag{3}$$

where μ is the viscosity of the fluid, the conservation of mass for the spreading current has the form (cf Barenblatt 1996; Fitzgerald & Woods, 1995)

$$r\frac{\partial h}{\partial t} = \frac{k\rho g}{\phi\mu}\frac{\partial}{\partial r}\left(rh\frac{\partial h}{\partial r}\right). \tag{4}$$

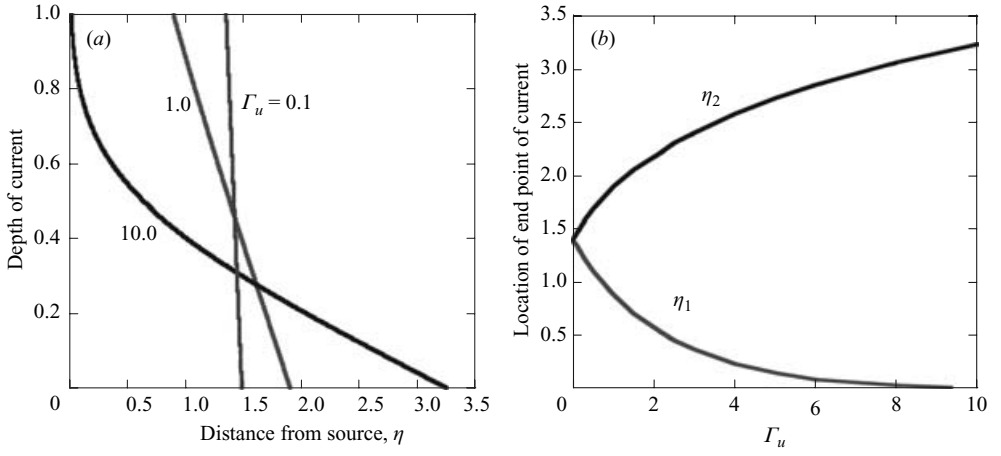

FIGURE 2. (*a*) The variation of the current depth with distance for a gravity intrusion advancing into an unsaturated porous layer. Curves are shown for three values of Γ_u: 0.1, 1.0 and 10.0, as labelled. (*b*) Prediction of the position of the front of the current in contact with the upper, η_1, and lower, η_2, surfaces of the aquifer as a function of Γ_u.

For the case of constant injection at the source, we seek solutions of the form $h = HF(\eta)$ where

$$\eta = \left(\frac{2\pi\phi H}{Qt}\right)^{1/2} r \tag{5}$$

and where F satisfies the shape equation

$$-\eta^2 F' = 2\Gamma_u(\eta F F')' \tag{6}$$

in the region $0 < F < 1$. Here Γ_u is defined as

$$\Gamma_u = \frac{2\pi k\rho g H^2}{\mu Q}. \tag{7}$$

In the limit of an infinitely deep aquifer, the current depth is singular at $\eta = 0$ (cf. Woods & Fitzgerald 1995). Therefore, for an aquifer of finite depth, we expect that the solution has the form

$$F = 1 \text{ for } 0 < \eta < \eta_1, \quad 0 < F < 1 \text{ for } \eta_1 < \eta < \eta_2, \quad F = 0 \text{ for } \eta > \eta_2, \tag{8}$$

and that it satisfies the boundary conditions that at $\eta = \eta_1$,

$$\eta_1 F' = -\frac{1}{\Gamma_u}, \tag{9}$$

and that at $\eta = \eta_2$, where $F = 0$, then

$$F' = -\frac{\eta_2}{2\Gamma_u}. \tag{10}$$

Numerical solution of the ordinary differential equation (6) combined with these boundary conditions identifies how the shape of the current depends on the single parameter Γ_u which is a measure of the rate of gravitational slumping compared to the rate of spreading associated with the fluid injection (figure 2*a*). As Γ_u increases, corresponding to a deeper layer, a lower injection rate, a higher permeability or a smaller viscosity of the invading fluid, then the current tends to slump along the base

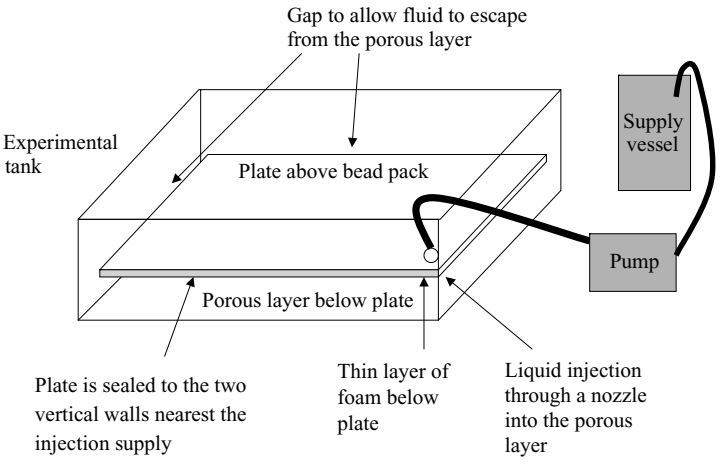

FIGURE 3. Schematic of the experimental system, consisting of a peristaltic pump, used to supply a constant flux of liquid to the bead pack below the upper horizontal plate.

of the cell, with $\eta_1 < \sqrt{2} < \eta_2$. In the fast injection limit $\Gamma_u = 0$, $\eta_1 = \eta_2 = \sqrt{2}$ (figure 2*b*), and the current behaves as if it is a pressure-driven flow. In the slow injection limit, $\Gamma_u \gg 1$, then $\eta_1 \to 0$ while $\eta_2 \sim (12\Gamma_u)^{1/4}$.

The predictions of the model for gravity-driven flow in a confined, unsaturated layer have been tested using a small-scale experimental model of a porous layer. The experimental tank was of horizontal dimensions 50 cm × 50 cm, and it was 20 cm deep (figure 3). A layer of glass beads, 3–5 cm in thickness, and of diameter 3 mm, was placed in the base of the tank. A lid, of size 49 × 49 cm, with a small hole drilled in one corner, was pressed down onto the glass beads, leaving a gap of 1 cm around two sides of the lid. The other two sides of the lid were sealed to the tank with putty, so that the small hole in the lid was located in the sealed corner between these two sealed sides of the lid. The lower surface of the lid was covered with a small layer of foam to reduce the permeability of the beads directly below the lid and thereby prevent short-circuiting of the fluid in the region directly under the lid. A systematic series of experiments was conducted using different values of the thickness of porous layer and the liquid injection rate, to cover a range of values of Γ_u in the range 0.01 to 1, corresponding to values of interest for practical situations (§ 6). In calculating Γ_u for the experiments, we estimated the value of the permeability of the bead pack using the results of Combarnous & Bories (1975); small changes in the packing of the glass ballotini from experiment to experiment may lead to small variations in this value, although by developing a repeatable packing procedure, we estimate that these fluctuations are less than 5 %.

Water was added to the bead pack through the hole near the sealed corner of the cell and this spread into the layer under gravity, fully flooding a zone near the source, and then slumping out along the base further from the source. The rate of advance of the front and the point of separation from the upper surface of the layer were recorded. In each experiment, both properties were found to spread at a rate proportional to $t^{1/2}$ as shown in figure 4(*a*), where the values of η_1 and η_2 (equation (8)) are shown as a function of time for three of the experiments. In figure 4(*b*) we compare the model predictions of η_1 and η_2 as a function of Γ_u, as obtained by numerical solution, with the experimental data. There is reasonable agreement between the

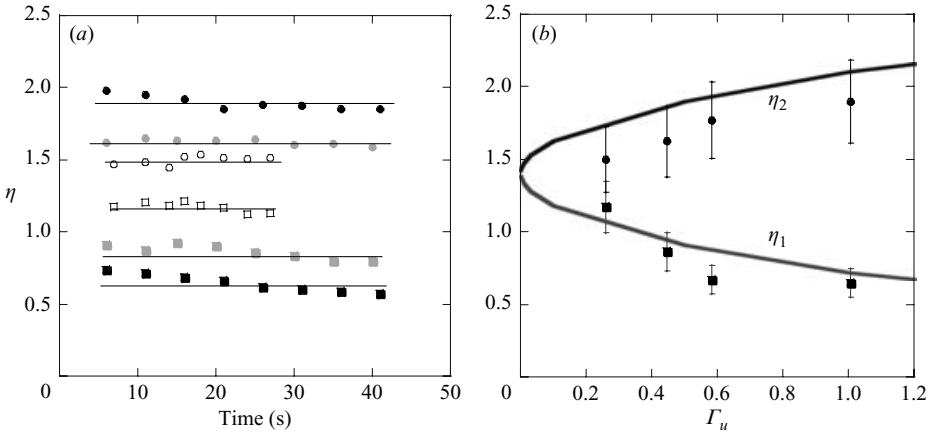

FIGURE 4. (*a*) Experimental measurements of η_1 (square symbols) and η_2 (circular symbols) as a function of time, for three experiments with Γ_u taking values 1.0 (black), 0.45 (grey) and 0.25 (hollow). (*b*) Comparison of η_1 (squares) and η_2 (circles) as a function of Γ_u as measured in the experiments and as predicted by the model (solid line). The error in the experimental data points is shown by error bars.

model predictions and the data, with some of the scatter in the frontal position resulting from local inhomogeneities in the bead pack.

3. Partially saturated layer

The analysis of § 2 can be readily extended to examine the case in which liquid is injected into a partially saturated aquifer. This situation may arise, for example, in a geothermal reservoir at saturation temperature, in which there is a layer of water at the base of the reservoir, and low-density vapour above (Elder 1981). Injection of more liquid into such a reservoir will lead to a gravitationally slumping current advancing into the existing layer of liquid. The far-field boundary condition now has the form

$$F \to \beta \quad \text{as} \quad \eta \to \infty \tag{11}$$

where $H\beta$ is the depth of the original layer of water in the aquifer, and $0 < \beta < 1$. This problem can be solved in an analogous fashion to that in § 2, using the same boundary condition at the point $\eta = \eta_1$ where $F(\eta_1) = 1$ (equation (9)), and the new boundary condition in the far field.

In figure 5(*a*), we illustrate how the shape of the current varies with the far-field fluid depth, β, for a given value of Γ_u, here chosen to be 3. It is seen that as the far-field depth increases, then the point of separation of the current migrates further from the source. This is a result of the outward displacement of the original fluid by the injected fluid: as the depth of the original fluid increases, there is more displaced fluid per unit radius of aquifer, and there is less space per unit radius to accommodate this fluid. Therefore, it tends to fully flood a larger zone of the reservoir. In figure 5(*b*), we show how the injection rate also affects the shape of the intruding fluid and the radius of the reservoir which becomes fully flooded. The figure presents a series of calculations to illustrate how the depth of the current adjusts as the buoyancy parameter Γ_u changes, for a fixed value of the far-field depth, $\beta = 0.16$. With a larger value of Γ_u, and hence a slower injection rate, the injected fluid spreads further into

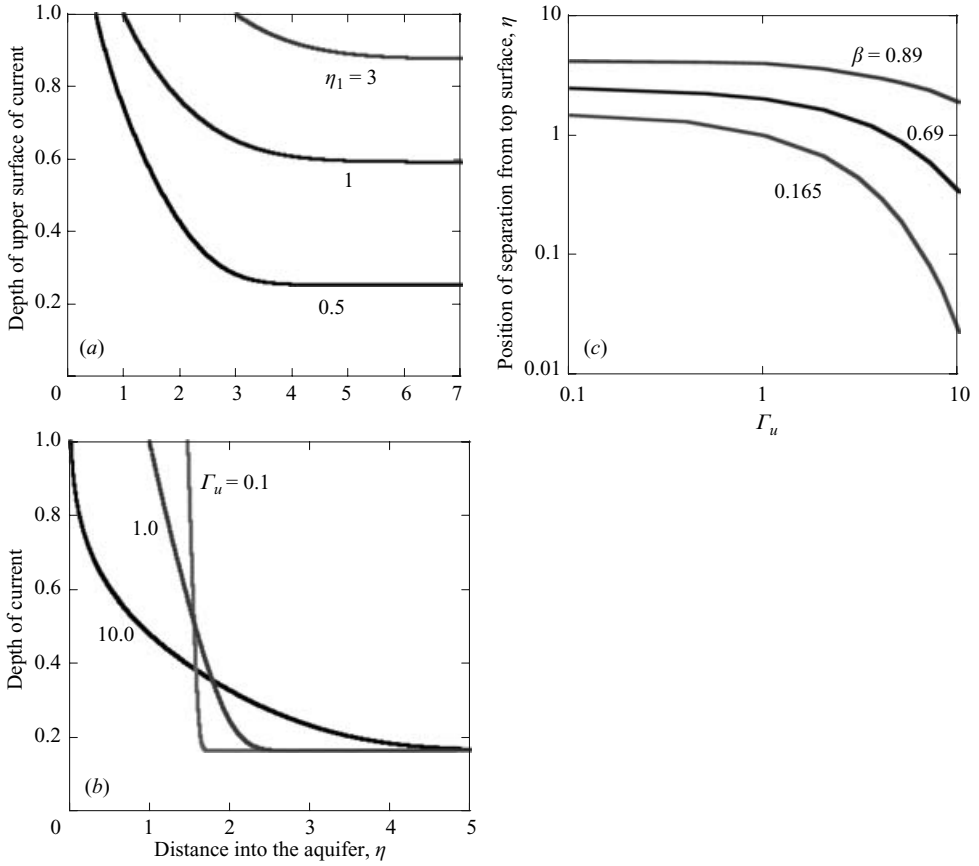

FIGURE 5. (*a*) Theoretical prediction of the depth of liquid as a function of radius as it is injected into a porous aquifer partially saturated with the same liquid. Curves are given for $\Gamma_u = 3$ and three values of the point of separation of the interface from the upper boundary of the aquifer, $\eta_1 = 0.5$, 1.0 and 3, as shown. These correspond to three values of the far-field depth of the liquid. (*b*) Variation of the shape of the upper surface of the current for three values of the parameter Γ_u: 0.1, 1.0 and 10.0, with the far-field depth of the fluid in the aquifer being fixed, $\beta = 0.16$. (*c*) Variation of the extent of the fully flooded zone near the injection well, η_1, as a function of Γ_u. Curves are given for three values of the far-field depth of the fluid in the aquifer.

the reservoir, and therefore there is a much narrower zone near the site of injection in which the reservoir becomes fully flooded. Figure 5(*c*) summarizes some of these principles through presentation of a series of calculations to illustrate how η_1 varies as a function of Γ_u for three different values of β. As expected, the point at which the current separates from the upper boundary of the aquifer occurs progressively further from the well as the original depth of water in the aquifer increases. Also, for a given value of this depth, the point of separation occurs further from the well as Γ_u decreases, owing to the decreasing impact of gravity in allowing the current to spread out; instead, if $\Gamma_u \ll 1$, then the current develops a sharp jump in depth at the radius $r(t)$ given by the point at which the volume of injected liquid Qt matches the volume available in the porous rock, above the original fluid, $\pi r^2 H(1-\beta)$.

4. Injection into a fully saturated aquifer

We now consider the case in which liquid of density ρ is injected into a horizontal, laterally extensive aquifer of depth H, porosity ϕ and permeability k, containing fluid of density $\rho - \Delta\rho$, with a flow rate Q from a central well (figure 1*c*). Again, we expect that once the flow has spread a distance greater than H from the well, so that the vertical pressure gradients are close to hydrostatic, then the flow properties become functions of radius, r, from the well, and the vertical pressure fluctuations are hydrostatic. However, in this situation, the original fluid in the aquifer also spreads radially from the source. If we denote the pressure on the base of the aquifer as $p_o(r, t)$ then assuming the vertical pressure gradient is hydrostatic, the pressure in the current has the form

$$p(r, z, t) = p_o(r) - \rho g y \quad \text{for } 0 < y < h, \tag{12}$$

$$p(r, z, t) = p_o(r) - \rho g h - (\rho - \Delta\rho) g (y - h) \quad \text{for } H > y > h. \tag{13}$$

Using radial symmetry, and Darcy's law for the horizontal component of the flow

$$u = -\frac{k}{\mu}\frac{\partial p}{\partial r}, \tag{14}$$

the conservation of mass for the lower layer of depth h locally has the form

$$r\frac{\partial h}{\partial t} = \frac{k}{\mu\phi}\frac{\partial}{\partial r}\left[rh\frac{\partial p_o}{\partial r}\right]. \tag{15}$$

If the fluid injection rate at the well is Q, then by mass conservation,

$$Q = -\frac{2\pi r k}{\mu}\left[H\frac{\partial p_o}{\partial r} - \Delta\rho g (H - h)\frac{\partial h}{\partial r}\right]. \tag{16}$$

With a constant injection rate, these equations reduce to the simpler form

$$r\frac{\partial h}{\partial t} + \frac{Q}{2\pi\phi H}\frac{\partial h}{\partial r} = \frac{k\Delta\rho g}{\mu\phi H}\frac{\partial}{\partial r}\left(rh(H - h)\frac{\partial h}{\partial r}\right). \tag{17}$$

This equation admits a solution of the form

$$h = HF(\eta) \quad \text{where} \quad \eta = r\left(\frac{2\pi\phi H}{Qt}\right)^{1/2} \tag{18}$$

and where

$$\left(1 - \frac{\eta^2}{2}\right)F' = \Gamma(\eta F(1 - F)F')'. \tag{19}$$

Here the parameter

$$\Gamma = \frac{2\pi k\Delta\rho g H^2}{\mu Q} \tag{20}$$

represents the balance between (i) the flow rate at which the injected liquid spreads under gravity through the original liquid and (ii) the flow rate associated with the injection of fluid at the well. For small Γ, we expect that the interface will be nearly vertical, but as Γ increases, the gravitational slumping becomes stronger, and the interface extends over a large range of radii (cf. § 2).

Since there is no flux of the original liquid at $\eta = 0$, we require $F = 1$ at $\eta = 0$. Thus, we seek solutions of the form

$$F = 1 \text{ for } 0 < \eta < \eta_1, \quad 0 < F < 1 \text{ for } \eta_1 < \eta < \eta_2, \quad F = 0 \text{ for } \eta > \eta_2. \tag{21}$$

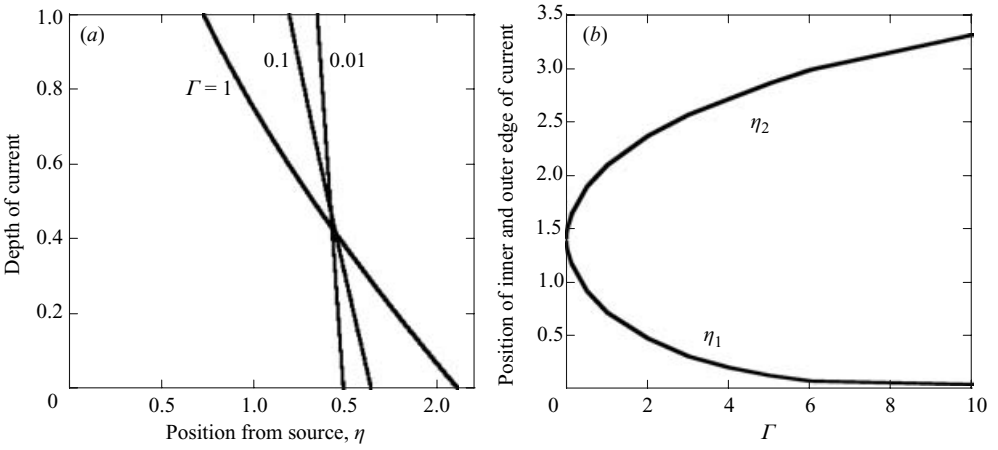

FIGURE 6. (*a*) Variation of the depth of a gravity intrusion advancing into a saturated porous layer as a function of distance, η. Curves are shown for three values of Γ: 1.0, 0.1 and 0.01, as labelled. (*b*) Variation of the position of the point of separation of the newly injected fluid from the upper surface of the aquifer η_1 and the lower surface of the aquifer η_2 as a function of Γ.

The boundary condition that $F=1$ at $\eta=\eta_1$ may be substituted into the governing equation (19) and this requires that

$$\frac{\mathrm{d}F}{\mathrm{d}\eta}=\frac{\eta_1^2-2}{2\Gamma\eta_1} \quad \text{at} \quad \eta=\eta_1. \tag{22}$$

Similarly, combining the boundary condition $F(\eta_2)=0$ at $\eta=\eta_2$ with the governing equation (19) implies that

$$\frac{\mathrm{d}F}{\mathrm{d}\eta}=\frac{2-\eta_2^2}{2\Gamma\eta_2}. \tag{23}$$

Numerical solution of (19) coupled with the boundary conditions (20)–(23) identifies how the interface becomes progressively more inclined as Γ increases (figure 6*a*). This corresponds to the effect of (i) increasing the density contrast, (ii) decreasing the flow rate, or (iii) increasing the permeability of the rock. The effect is corroborated in figure 6(*b*) in which we illustrate how η_1 decreases while η_2 increases with Γ. Note that, in our dimensionless formulation, the limiting case $\Gamma\to 0$ leads to the purely pressure-driven flow $\eta_1=\eta_2=\sqrt{2}$, and so by conservation of mass, in general $\eta_1\leqslant\sqrt{2}\leqslant\eta_2$.

The theoretical predictions of the variation of η_1 and η_2 with Γ have been tested experimentally using the same small-scale experimental model of § 2. In this case however, the tank was saturated with fresh water prior to the injection of a relatively saline solution through the corner hole. A systematic series of experiments was conducted using different values of the salinity and hence buoyancy of the injected liquid and different values for the flow rate, thereby producing a range of values of Γ, $0.001<\Gamma<1$, corresponding to values of interest for practical situations (§ 6).

In each experiment, the fluid again spreads out approximately radially from the sealed corner of the tank, advancing more rapidly over the lower surface of the tank. The position of the flow front and the point of separation of the current from the upper surface of the tank was recorded at a series of times by photographing the current from the side and from below, and then determining the mean radius of the flow from

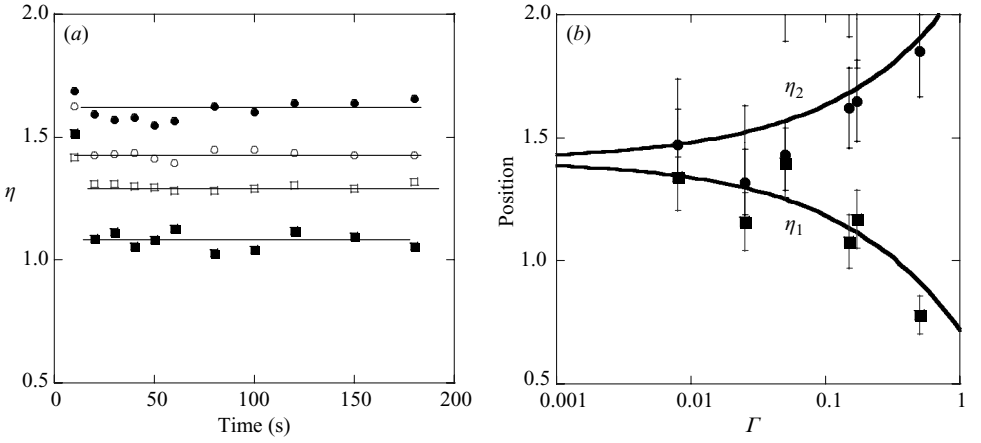

FIGURE 7. (*a*) Variation of the measured values η_1 (square symbols) and η_2 (circular symbols) as a function of time illustrating that the flow is indeed self-similar. Data are shown for two experiments, in which Γ took the values 0.15 (solid symbols) and 0.008 (hollow symbols). (*b*) Variation of the location of the point at which the current separates from both the upper, η_1, and lower, η_2, surfaces of the confining porous aquifer, as a function of Γ. The theoretical predictions (curves) are compared with the experimental observations, with square symbols corresponding to η_1 and round symbols corresponding to η_2.

the images. Owing to the solid base, the permeability is somewhat larger in a zone of thickness comparable to the radius of the glass ballotini, adjacent to the base, than in the main bead pack. As a result, the current tends to disperse through this high-permeability zone a little faster than the main front. In estimating the effective leading edge of the current, we have corrected the data for this additional dispersion by using the cross-sectional profile of the current on the sidewall of the tank to estimate where the leading edge would be without the small dispersed zone at the base of the cell. In figure 7(*a*), we compare the experimental measurements of η corresponding to (i) the position of the point of separation of the current from the upper surface, and (ii) the location of the leading edge of the current, as a function of time. Again, the currents spread at a rate proportional to $t^{1/2}$. We compare the measured values of η_1 and η_2 with the theoretical predictions of the model in figure 7(*b*). There is reasonably good agreement between the model and the data, especially considering the approximations implicit in the model, and the small scale of the experimental model.

5. Discussion

It is interesting to note that we can merge the results of §§2, 3 and 4 to describe the case in which dense fluid is injected into an aquifer which is partially saturated with water of lower density (figure 1*d*). The solutions presented in §§2–4 apply together under the condition that the interface between the new fluid and the original aquifer fluid, at the base of the layer, advances more slowly than the point at which the fluid separates from the upper layer of the aquifer (figure 8, region above the line). In this situation, the motion is governed by the solutions described in §4 up to the leading edge of the newly injected fluid on the base of the layer. Beyond this, the motion is governed by the solutions described in §3 and depend on the far-field depth of the fluid, β.

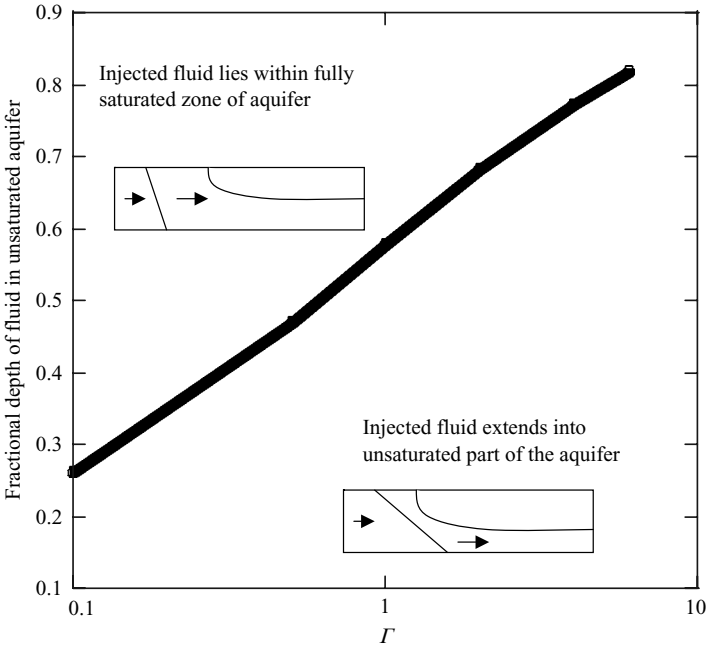

FIGURE 8. Regime diagram illustrating the critical far-field depth of the fluid in the aquifer as a function of Γ for which the present solutions describe the injection of fluid of one density into an unsaturated permeable layer of a second density. In this calculation, the density contrast between the upper and lower layers is a fraction 0.01 of the lower layer density. With smaller values of the far-field depth, or larger values of Γ than given by the critical curve, the new fluid slumps out radially beyond the point of separation of the fluid from the upper surface of the aquifer, as indicated in the figure.

By combining the solutions and taking a particular density ratio between the original and new fluid, Γ/Γ_u, then for each value of β, the far-field depth of the liquid, we can calculate the maximum value of Γ for which the newly injected dense fluid remains in that part of the aquifer which is fully flooded. As an example, we present the locus of these maximum values of Γ for the case $\Gamma/\Gamma_u = 0.01$ in figure 8. It is seen that unless the aquifer has only a small initial depth of water, then for realistic values of $\Gamma < 0.1$ (see § 6) it is unlikely that the injected liquid will extend beyond the fully saturated part of the aquifer (figure 8).

6. Summary

In summary, we have presented a series of new similarity solutions to describe the injection of liquid into a confined and partially saturated aquifer. We have successfully tested the model with some new laboratory experiments. If the injection fluid has the same density as the original fluid, and the aquifer is only partially saturated, then the key controlling parameter is Γ_u, the ratio of the gravity-driven flow speed to the pressure-driven flow speed. In schemes in which fresh water is injected into an aquifer the permeability may typically have value 0.01–1.0 Darcy, and the vertical extent of the aquifer is of order 10–100 m. With typical injection rates of order 0.001–0.1 $\mathrm{m^2\,s^{-1}}$, Γ_u may then have value of order 10^{-3}–10^2. We deduce that unless the injection rate is slow, or the aquifer is very permeable or deep, then $\Gamma_u < 1$ and the pressure-driven flow dominates the dynamics. However, even in that case, the

self-similar model does predict some slumping of the current. In an initially unsaturated aquifer the distance between the region which is fully flooded with injected fluid, and the leading front of the injected fluid, spreads as $(\eta_2 - \eta_1)(Qt/2\pi\phi H)^{1/2}$. This zone thereby becomes progressively more inclined towards the horizontal. Indeed, our calculations with $\Gamma_u \sim 0.01$–0.1 (figure 4*b*), show that this inclined zone may represent upto 30 % of the total radial extent of the flow.

If the aquifer is initially saturated with less dense fluid than that being injected, then the dimensionless buoyancy-driven flow parameter, Γ, controls the flow dynamics. With typical parameters, $10^{-5} < \Gamma < 10^{-2}$, then figure 7 illustrates that the interface between the newly injected and original fluid extends for less than a few percent of the total extent of the current.

In the present work, we have assumed that any viscosity differences between the fluids is relatively small and that the fluids are miscible. These assumptions are appropriate approximations for the problem of fresh water injection into a saline aquifer, or the process of water injection into a geothermal reservoir. However, it is important to recognize that in the case of water injection into an oil reservoir, or CO_2 injection into an aquifer, there may be substantial contrasts in the fluid viscosity, as well as density. Also, the interfacial tension between the phases can lead to two-phase flow effects and the formation of Buckley–Leverett discontinuities in fluid saturation (Bear 1972). We plan to extend the present modelling and experimental approach to determine conditions under which it can also account for these additional phenomena.

V. M. thanks the Churchill Foundation of the United States of America for her Studentship.

REFERENCES

Barenblatt, G. I. 1996 *Scaling, Self-Similarity, and Intermediate Asymptotics*. Cambridge University Press.

Bear, J. 1972 *Dynamics of Fluids in Porous Media*. Elsevier.

Combarnous, M. A. & Bories, S. A. 1975 *Hydrothermal Convection in Saturated Porous Media: Advances in Hydroscience*. Academic.

Elder, J. 1981 *Geothermal Systems*. Academic.

Fitzgerald, S. D. & Woods, A. W. 1995 Vapour flow in a hot porous rock. *J. Fluid Mech.* **293**, 45–65.

Henry, H. R. 1964 Interfaces between saltwater and fresh water in coastal aquifer. *USGS Water Supply Papers*.

Homsy, B. 1987 Viscous fingering in porous media. *Annu. Revi. Fluid Mech.* **19**, 271.

Huppert, H. E. & Woods, A. W. 1995 Gravity driven flow in porous layers. *J. Fluid Mech.* **292**, 55–69.

Menand, T. & Woods, A. W. 2005 Dispersion, scale and time-dependence of mixing zones under gravity stable and unstable dsplacements in porous media. *Water Resour. Res.* **41**, W05014.

Reese, R. S. 2001 Inventory and review of aquifer storage and recovery in southern Florida. *USGS Water Resources I Investigations Report*.

Woods, A. W. 1999 Liquid and vapour flows in superheated rock. *Annu. Rev. Fluid Mech.* **31**, 171–199.

Woods, A. W. & Mason, R. 2000 The dynamics of two layer gravity driven flows in permeable rocks. *J. Fluid Mech.* **421**, 83–114.